

Improvement of Photoreceptor Function Following Transplantation of NS-Derived RPE Cells into the Subretinal Space of an Animal (Rat) Model of Retinal Degeneration

Hamid Aboutaleb Kakhodaieian^{1,2}, Taki Tiraihi^{1*}, Hamid Ahmadi³, Hossein Ziaei³, Narsis Daftarian⁴ and Taher Taheri⁵

¹Department of Anatomical Sciences, Faculty of Medical Sciences, Tarbiat Modares University, Tehran, Iran

²Department of Anatomical Sciences, Faculty of Medicine, Semnan University of Medical Sciences, Semnan, Iran

³Ophthalmic Research Center, Research Institute for Ophthalmology and Vision Science, Shahid Beheshti University of Medical Sciences, Tehran, Iran

⁴Ocular Tissue Engineering Research Center, Research Institute for Ophthalmology and Vision Science, Shahid Beheshti University of Medical Sciences, Tehran, Iran

⁵Shefa Neuroscience Research Center, Khatam-Alanbia Hospital, Rashid Yasemi Street, Tehran, Iran

*Corresponding Author: Taki Tiraihi, Department of Anatomical Sciences, Faculty of Medical Sciences, Tarbiat Modares University, Tehran, Iran.

Received: June 22, 2022

Published: July 19, 2022

© All rights are reserved by Taki Tiraihi, et al.

Abstract

Purpose: To investigate transplantation of retinal pigment epithelium (RPE) antigen (PSRA)-expressing pigmented spheres in an animal (rat) model of age-related macular degeneration (AMD) using sodium iodate to rescue and improve (i) a- and b-wave activities, (ii) alter outer nuclear layer thickness, and (iii) enhance cell number.

Materials and Methods: Male hooded rats (n = 65) were divided into five groups, two of which received sodium iodate and three of which did not. AMD was induced using retro-orbital sodium iodate injection. After 30 days, cells were injected into the subretinal space using a trans-scleral approach. For cell transplantation, rat bone marrow stromal stem cells were differentiated into neurospheres (NSs) and, after 7 days, into RPE cells. For tracking, differentiated cells were labeled with BrdU and then transplanted into the subretinal space. Photoreceptor function was evaluated by full-field electroretinography over the course of 7-90 days. The effects of transplanted cells on neurosensory retina and RPE layer were assessed using immunohistochemistry and cresyl violet staining at corresponding time points.

Results: Both the scotopic b-wave at an intensity of 0.01 cd.s/m² and photopic a-wave at an intensity of 3.0 cd.s/m² were affected. Significant differences between the test groups and relevant controls appeared at 60 days, but only for the scotopic assay and, at 90 days, for the photopic assay. Seven days after injection, light microscopy of IHC on paraffin sections in the transplanted group showed that PSRA cells had migrated and integrated into the host RPE layers. Further investigation using specific RPE cell protein RPE65 and ZO-1 revealed that these cells were able to express specific proteins as well. There was a statistically significant difference between the numbers of outer nuclear layer (ONL) cells and thicknesses in transplanted group. Significant differences between the test group and relevant controls appeared throughout the 7-90 day course in ONL cell count and through 14-90 days in ONL thickness. Ninety

days after transplantation, the RPE layer and the neurosensory retinal layers were detectable. There was a surprising affinity between the PSRA cells and the host RPE layer.

Discussion: We demonstrated that PSRA migrated into the subretinal space and integrated into the host layer, expressing ZO-1, and RPE65 markers. Additionally, we showed that photoreceptor activity improved. The ONL was thicker, and ONL cell numbers were better preserved than in RPE-damaged rats that received only phosphate buffered saline (PBS).

Keywords: Photoreceptor Function; RPE; Subretinal Space; Sodium Iodate; Rat BMSCs

Introduction

Cell therapy is a most promising treatment for degenerative eye diseases, including age-related macular degeneration (AMD), retinitis pigmentosa (RP), and Stargardt disease (SD), all of which are common conditions involving one or more cell types, impairment of any of which results in disorders of retinal function [1]. AMD is a multifactorial disorder, and fundamental and environmental factors accelerate its development [2]. The probability of its occurrence increases with age and manifests as wet or dry forms. In the former, neovascularization of the choroidal layer subjacent to the RPE occurs, and invades the subretinal space, leading to loss of central vision. In the latter, a disturbance in RPE function causes accumulation of drusen [3] in Bruch's membrane (BM), which lies between the choroid and RPE. Hence, BM thickness increases [4], resulting in reduced oxygenation and decreased nutrition of the RPE and photoreceptors [5].

The RPE comprises a monolayer of epithelial cells lying between the neurosensory retina and choroid [5]. The basal portions of these polarized cells are located on BM, while the apical portions are in contact with photoreceptors. RPE cells are directly responsible for retinal health, with a variety of functions associated with the neurosensory retina and choroid. Some of the RPE's essential primary daily functions are that of (i) phagocytosis of photoreceptor outer segments, resulting in their rebuilding, and (ii) completion of the visual cycle (all-trans retinol to 11-cis-retinal). Consequently, RPE assures the quality of the sensory retina and visual system. The critical roles of RPE cells in AMD, RP, and SD are well known [6]. As AMD progresses, RPE cells become hypo-pigmented and degenerative, resulting in photoreceptor and, ultimately, bipolar cell injury [7].

To date, there is no effective treatment for dry AMD [8], although RPE replacement therapy is a promising modality [5].

Such treatment is in clinical and preclinical trial phases of animal model investigations. Wet and dry AMD clinical trials have made use of a variety of stem cells—embryonic, induced pluripotent, and adult mesenchymal stem cells (MSCs)—as well as various cell lines—ARPE-19, autologous RPE, and exogenous RPE [9]. In these strategies, cells have been implanted as suspensions or monolayers [5].

MSCs appear to be safe to use for replacement therapy [10], as they produce diverse neuroprotective factors and cytokines. In addition, they are able to differentiate into mesodermal, neural, and epithelial lineage cells. In previous studies, we showed that rat bone marrow stromal stem cells (BMSCs) [11], and rat and human adipose-derived stem cells (ADSCs) [12] differentiated into neurospheres (NS), neural stem cells (NSCs), RPE, and even retinal cells (data not shown). Transplantation of MSCs-NSs in the rat RPE degeneration model resulted in the rescue of RPE and ONL cells [13]. Because vision can be lost following RPE and photoreceptor cell injury, one of the most critical goals of cell replacement therapy in AMD is the rescue of RPE cells and improvement of photoreceptor activity.

Several studies have specifically investigated photoreceptor, bipolar, and ganglion cell function after cell replacement therapy [14]. In a previous study, we showed that sodium iodate resulted in disruption of the electrical activity of photoreceptors, as disclosed by electroretinography (ERG) in a- and b-wave amplitudes [15].

Because of the potential of MSCs-NS to differentiate into both RPE and progenitor- expressing OTX2 cells, we investigated the hypothesis that transplantation of PSRA in an AMD model using sodium iodate can improve a- and b-wave activity, and increase ONL thickness and cell number.

Materials and Methods

Animals

Male hooded rats (n = 65) (Razi Institute, Iran, Tehran), weighing 250-300 g were divided into five groups, comprising control (n = 13) = no-sodium iodate; AMD/PSRA (n = 13) = sodium iodate (40 mg/kg) and 28 days later, PSRA injected into the sub-retinal space; AMD/PBS (n = 13 = sodium iodate and 28 days later PBS injected into the subretinal space; NO AMD/PBS (n = 13) = no-sodium

iodate and PBS injected into the sub-retinal space; ROS/PBS (n = 13) = no-sodium iodate and PBS injected into the retro-orbital sinus. Animals were housed under standard laboratory conditions: 12-h light/dark cycles at 20°C. All experimental procedures were performed in accordance with ARVO guidelines for the use of animals in ophthalmic and vision research. The study was approved by the Ethics Committee of Tarbiat Modares University, Tehran, Iran.

Groups					
	Control	AMD/RPE	AMD/PBS	NO AMD/PBS	ROS/PBS
Sodium iodate	-	+	+	-	-
PSRA Cell	-	+	-	-	-
PBS	-	-	+	+	+

Table a

RPE injury model

To achieve the RPE injury model, a retro-orbital sinus injection was performed, as previously described [13]. In brief, sodium iodate (Sigma-Aldrich, CAS Number 7681-55-2, Linear Formula: sodium iodate, MW:197.89, Steinheim, Germany) was diluted in sterile phosphate-buffered saline (PBS) to a final concentration of 5%, filtered, adjusted to pH 7.2 and kept at 4°C. For experimental groups (AMD/PSRA and AMD/PBS), 40 mg/kg sodium iodate was injected into the left retro-orbital sinus. Anesthetized animals were positioned on a warm pad (25°C) and placed in a lateral anatomical position, with the left eye facing up. A 30-gauge, 1-in insulin needle was inserted into the medial canthus, deep into the vessels behind the eye, at a 45° angle to the nose. Sodium iodate was injected gently into the retro-orbital sinus vessels. After completion of the injection, the needle was withdrawn slowly, and light pressure was applied to prevent bleeding.

Cell culture and differentiation

Generation of RPE cells from the NSs was performed, as previously described [11]. In brief, third-passage harvested rat BMSCs were seeded (10⁴ cells/cm²) into a NS medium ((DMEM/F12), supplemented with 20 ng/ml EGF (Sigma-Aldrich, Steinheim, Germany), 20 ng/ml of essential fibroblast growth factor (bFGF; Chemicon, Hofheim, Germany, and 2% B27 (Invitrogen, Karlsruhe, Germany))-containing six-well plate NSs were incubated for an additional 2 days in NS medium and then replaced with differentiation medium—low glucose DMEM with 1% fetal bovine

serum (FBS), penicillin/streptomycin and PSRA cocktail: 1.4 x 10⁻⁸ M selenous acid, 2.8 x10⁻⁸ M hydrocortisone, 3 x10⁻⁷ M linoleic acid, 8.3 x 10⁻⁷ M insulin, 6 x 10⁻⁸ M transferrin, 2. x 10⁻⁶ M putrescine, and 10⁻¹¹ M triiodothyronine —and incubated for 15 days with RPE spheres. For distinguishing host from transplanted cells, BrdU (5-bromo-2'-deoxyuridine) was added to the culture medium at a concentration of 7.81 µl/ 2.5 ml and incubated at 37°C for 72 hr. Labeled PSRA in culture media (containing factors to stimulate RPE differentiation) was prepared for subretinal transplantation.

Transplantation of PSRA(s) into the subretinal space

Trans-scleral subretinal injection through the posterior portion of the sclera was performed, as previously described [16]. Subretinal injections (PSRA or PBS) made into the left eye were performed in groups AMD/PSRA, AMD/PBS, NO AMD/PBS, but not ROS/PBS. In brief, rats were anesthetized 2% pentobarbital i.p. (40 mg/kg; Santen, Osaka, Japan) and topical 1% proparacaine eye drops (Santen). Pupillary dilation was achieved with 0.5% tropicamide and 0.5% phenylephrine eye drops (Santen). After complete dilation, anesthetized animals were placed in a lateral anatomical position under a dissecting microscope (Zeiss) and held with a hand. The fundus was visualized with the application of a drop of 2.5% methylcellulose. A small incision was made on the posterior pole of the sclera, and subjacent layers were gently and individually pulled back to reach the sclera. At this time, a blunt 30-gauge Hamilton needle tip (Hamilton Company, Reno, Nevada, USA) was inserted through the puncture and advanced into the subretinal space. The syringe was held in place and 3µL

PSRA suspension (10^5 cells/ml) containing RPE spheres in culture media slowly injected for ~30 s. After subretinal delivery, the needle was gently withdrawn, and the injection site sutured. Post-surgery, bacitracin, neomycin, and polymyxins were applied locally to protect the eye.

Electroretinography

Full-field ERG recordings of scotopic and photopic flash, with contact-lens gold-wire loop electrodes (Metrovision, France) were made for all rats ($n = 65$ eyes). The time chosen for ERG recording was 28 days after sodium iodate injection—b- and a-waves have been reported to decline at that time [15]—allowing transplantation effects to be identified judiciously. Scotopic and photopic full-field, using Ganzfeld bowl light stimulation (Metrovision, France), were recorded in each group at seven ($n = 13$ animals), fourteen ($n = 14$ animals), thirty ($n = 9$ animals), sixty ($n = 7$ animals), and ninety ($n = 5$ animals) days after PSRA transplantation, as previously described [15]. Animals were kept in a dark room for at least 1 hour for dark adaptation, after which they were anesthetized with an injection of ketamine i.p. (40 mg/kg) and xylazine (4 mg/kg) (Alfasan Company, Woerden, the Netherlands). The cornea was numbed using alcaine (Alcon, Fort Worth, Texas, USA), and the pupils were dilated with 1% atropine (Sina, Tehran Iran) in dim red light. Scotopic recordings were performed under dark conditions under dim red light at light intensities of 0.01, 3.0, and 10 candela (cd) x steradian (s) per square meter ($\text{cd}\cdot\text{s}/\text{m}^2$) to elicit maximal rod, combined rod, and cone responses. After light adaptation for 10 min, photopic ERGs were elicited using a $3.0 \text{ cd}\cdot\text{s}/\text{m}^2$ light intensity on a white background of $30 \text{ cd}/\text{m}^2$. For each recording, five different responses were averaged by an ERG recording system (RETI port 21, version: 19-99-04-7.2E, Roland Consult, Electrophysiologic Diagnostic System, D-14770 Brandenburg, Germany). Results are shown as a- and b-wave amplitudes in microvolts.

Histology

Seven, 14, 30, 60, and 90 days of recording ERGs, eyes were enucleated from two rats randomly chosen from each group. These animals were euthanized under deep anesthesia (ketamine/xylazine at 500/50 mg/kg i.p.), during which time the eyes were enucleated and fixed in paraformaldehyde 4% for 2 hr at 4°C . Corneas, lenses, and neural retinas were removed from each fixed eye. For light microscopy, fixed eyes embedded in paraffin. We cut $5\text{-}\mu\text{m}$ thick retinal sections in the nasotemporal plane through the optic nerve and the center of the cornea. For descriptive histology and quantitative analysis, sections were stained with crysel violet

staining. All observations and photography were performed using a fluorescent microscope (BX41; Olympus Corp., Tokyo, Japan) equipped with a digital camera (DP70; Olympus Corp.). Image processing and quantification were performed using a software (Photoshop CS7; Adobe Systems, Mountain View, CA, USA) and image analysis software (ImageJ 1.46r; Wayne Rasband, National Institutes of Health, USA, <http://imagej.nih.gov/ij>).

Immunohistochemistry

For whole-mounts, four radial cuts were made in each eye cup. Auto-fluorescence microscopy was performed using an excitation wavelength of $>498 \text{ nm}$ of the RPE sheet before immunohistochemistry with an autofluorescence microscope (BX41; Olympus Corp., Tokyo, Japan) equipped with a digital camera (DP70; Olympus Corp.).

For cross section immunohistochemistry, deparaffinized sections were blocked with PBS solution containing 1% bovine serum albumin, 0.1% Triton X-100, and 10% normal horse serum, and subsequently incubated overnight at 4°C with primary antibodies (Table 1). After washing in PBS, sections were incubated for 1 hour at room temperature with one of the following secondary antibodies goat anti-mouse and goat anti-rabbit secondary antibodies conjugated with FITC. To determine the specificity of the antigen-antibody reaction, corresponding negative controls with the secondary antibody alone were performed.

For BrdU detection, sections were re-hydrated and, after antigen retrieval with trypsin, sections were first incubated with primary anti-BrdU 2 h at room temperature, and then incubated with secondary anti-BrdU conjugated with Alexa fluor 594 (Sigma-Aldrich, Steinheim, Germany) 1 h in RT. After rinsing, observed by fluorescence microscopy (BX41; Olympus Corp., Tokyo, Japan) equipped with a digital camera (DP70; Olympus Corp.).

Statistical analyses

Data were obtained and expressed in mean \pm SEM values. The data were tested for normality using the Kolmogorov-Smirnov test. All data showed no departure from a normal distribution. ERG peaks between groups were analyzed with ordinary one-way analysis of variance (ANOVA), Tukey's multiple comparison, and comparisons between all groups. For analysis between two groups, unpaired two-tailed *t*-test by GraphPad Prism (Version 8, GraphPad Prism Inc., San Diego, California, USA) was used. Statistical significance was set at $p < 0.05$.

Primary antibody	Host	Titer	Cell	Supplier
Anti-Rpe65	Mouse	1:200	Retinal pigment epithelium cell	Abcam, Cambridge, UK
Anti-ZO-1	Rabbit	1:200	Tight junction	Abcam, Cambridge, UK
Anti-BrdU	Mouse	1:200	Dividing at the time of BrdU application	Abcam, Cambridge, UK
Goat anti-mouse secondary antibodies	Goat	1:500	Reacted with mouse primary antibody	Abcam, Cambridge, UK
Goat anti-rabbit secondary antibodies	Goat	1:500	Reacted with rabbit primary antibody	Abcam, Cambridge, UK
Alexa fluor 594		1:500	BrdU labeled PSRA	Sigma-Aldrich

Table 1: The primary antibodies cross react with rat host cells and transplanted cells.

Statistical analysis and electroretinography

ERG 7, 14, 30, and 90 days indicated that the only effect was on the scotopic b-wave—at a light intensity of 0.01 cd.s/m² — and

photopic a-wave, at a light intensity of 3.0 cd.s/m² (supplementary tables 2, 8). Figure 1 illustrates the events occurring during the recordings.

Figure 1: A: RPE differentiated from bone marrow stromal stem cells. B: Schema reveals how the NS-derived RPE-like cells transplanted into the subretinal space. C: ERG of eyeball received transplanted RPE-like sphere cells into the subretinal space. D: Schema of the retina defines the rod and cone photoreceptors, bipolar, and third-order neurons affected by various intensities. Dark-adaptation (black panel), ON bipolar cells transmit light on their own (ON1) and through cells (ON2). By increasing the stimulus (middle panels), ON bipolar cells transmit light by ON-bipolar (ON1, ON2) and S cone cells to ON ganglionic cells. Light-adaptation (white panel), the S cone and M/S Co-expressing cones are responsible for transmitting stimuli to ON ganglionic cells. Abbreviations; RPE: retinal pigment epithelium, ONL: outer nuclear layer, INL: inner nuclear layer, SC: scleral layer, CC: Choriocapillaris, GL: ganglion cell layer, POS: photoreceptors outer segment, OPL: outer plexiform layer, IPL: inner plexiform layer, ON: optic nerve, R: Rod photoreceptor, C: Cone photoreceptor, RB: Rod bipolar cell, AII, A17: Amacrine cells, CB: Cone bipolar cell, GC: Ganglionic cell.

Analysis of variance (ANOVA) of ERG indicated that at 7 days post-transplantation, the a-wave intensities observed in the experimental groups were not significantly different; there was also no significant difference in b-wave intensities observed in different groups (supplementary tables 3-7 and Figure 2).

However, there was a statistically significance difference between all groups in b-wave amplitude (scotopic 0.01 cd.s/m², scotopic 3.0 cd.s/m² after 14, 30, and 60 days) and between all groups in a-wave amplitude (scotopic 10.0 cd.s/m² and photopic 3.0 cd.s/m²) after 90 days (Supplementary tables 1-3, 7, 8).



Intensity mV	Scotopic b-wave 0.01 cd.s/m ²		Scotopic b-wave 3.0 cd.s/m ²		Scotopic b-wave 10.0 cd.s/m ²		Photopic b-wave 3.0 cd.s/m ²		Scotopic a-wave 3.0 cd.s/m ²		Scotopic a-wave 10.0 cd.s/m ²		Photopic a-wave 3.0 cd.s/m ²	
	-	P =	-	P =	-	P =	-	P =	-	P =	-	P =	-	P =
7 days	-	P = 0.4264	-	P = 0.0673	-	P = 0.4354	-	P = 0.7377	-	P = 0.5236	-	P = 0.0993	-	P = 0.7902
14 days	+	P = 0.0264	+	P = 0.0354	-	P = 0.4683	-	P = 0.3550	-	P = 0.3133	-	P = 0.0811	-	P = 0.4678
30 days	+	P = 0.0182	-	P = 0.0673	-	P = 0.3121	-	P = 0.6498	-	P = 0.0705	-	P = 0.1317	-	P = 0.4799
60 days	****	P < 0.0001	-	P = 0.6524	-	P = 0.8586	-	P = 0.6426	-	P = 0.5411	-	P = 0.2491	-	P = 0.7663
90 days	-	P = 0.4794	-	P = 0.1503	-	P = 0.4677	-	P = 0.7792	-	P = 0.0909	+	P = 0.0416	**	P = 0.0023

Supplementary Table 1: Data analysis (ANOVA) of the a- and b-wave intensities in all days.

Tukey's multiple comparisons test	7 Days P = 0.4264		14 Days P = 0.0264*		30 Days P = 0.0182*		60 Days P < 0.0001****		90 Days P = 0.4794	
	Significant	Adjusted P Value	Significant	Adjusted P Value	Significant	Adjusted P Value	Significant	Adjusted P Value	Significant	Adjusted P Value
Control vs. AMD/PSRA	ns	0.6214	ns	0.9464	*	0.0353	**	0.0083	ns	0.9666
Control vs. AMD/PBS	ns	0.8588	ns	0.9863	ns	0.138	ns	0.2484	ns	0.9997
Control vs. NO AMD/PBS	ns	0.6916	ns	0.096	ns	0.35	ns	0.4933	ns	>0.9999
Control vs. ROS/PBS	ns	0.3409	ns	0.9876	*	0.0129	*	0.015	ns	0.5798
AMD/PSRA vs. AMD/PBS	ns	0.9846	ns	0.9981	ns	0.8805	****	<0.0001	ns	0.9202
AMD/PSRA vs. NO AMD/PBS	ns	0.9996	*	0.0469	ns	0.9394	***	0.0003	ns	0.9849
AMD/PSRA vs. ROS/PBS	ns	0.9927	ns	0.7769	ns	0.9965	****	<0.0001	ns	0.9069
AMD/PBS vs. NO AMD/PBS	ns	0.9968	*	0.0362	ns	>0.9999	ns	0.9934	ns	0.9978
AMD/PBS vs. ROS/PBS	ns	0.8537	ns	0.8575	ns	0.663	ns	0.5205	ns	0.4734
NO AMD/PBS vs. ROS/PBS	ns	0.9633	ns	0.2249	ns	0.8234	ns	0.3471	ns	0.6533

Supplementary Table 2: Data analysis (ANOVA) of the b-wave Scotopic 0.01 cd.d.m² in all different groups.

Tukey's multiple comparisons test	7 Days P = 0.6483		14 Days P = 0.0354*		30 Days P = 0.0673		60 Days P = 0.6524		90 Days P = 0.1503	
	Significant	Adjusted P Value	Significant	Adjusted P Value	Significant	Adjusted P Value	Significant	Adjusted P Value	Significant	Adjusted P Value
Control vs. AMD/PSRA	ns	0.9992	ns	0.52	ns	0.0898	ns	>0.9999	ns	0.9115
Control vs. AMD/PBS	ns	0.9997	ns	0.7789	ns	0.1005	ns	0.8753	ns	0.9248
Control vs. NO AMD/PBS	ns	0.9601	ns	0.6106	ns	0.8006	ns	>0.9999	ns	0.4296
Control vs. ROS/PBS	ns	0.7819	ns	0.8282	ns	0.1123	ns	0.822	ns	0.8256
AMD/PSRA vs. AMD/PBS	ns	0.9916	ns	0.9736	ns	0.9995	ns	0.9104	ns	0.4891

AMD/PSRA vs. NO AMD/PBS	ns	0.9929	ns	0.0714	ns	0.7768	ns	0.9998	ns	0.8872
AMD/PSRA vs. ROS/PBS	ns	0.8964	ns	0.1337	ns	0.9986	ns	0.8645	ns	0.9995
AMD/PBS vs. NO AMD/PBS	ns	0.8887	ns	0.1143	ns	0.8413	ns	0.8419	ns	0.1275
AMD/PBS vs. ROS/PBS	ns	0.6282	ns	0.2239	ns	>0.9999	ns	>0.9999	ns	0.3774
NO AMD/PBS vs. ROS/PBS	ns	0.9863	ns	0.9947	ns	0.8638	ns	0.7831	ns	0.9522

Supplementary Table 3: Data analysis (ANOVA) of the b-wave Scotopic 3.0 cd.d.m² in all different groups.

Tukey's multiple comparisons test	7 Days P = 0.4354		14 Days P = 0.4683		30 Days P = 0.3121		60 Days P = 0.8586		90 Days P = 0.4677	
	Significant	Adjusted P Value	Significant	Adjusted P Value	Significant	Adjusted P Value	Significant	Adjusted P Value	Significant	Adjusted P Value
Control vs. AMD/PSRA	ns	0.999	ns	0.9508	ns	0.6254	ns	>0.9999	ns	0.7547
Control vs. AMD/PBS	ns	0.9938	ns	0.9983	ns	0.6972	ns	>0.9999	ns	0.9497
Control vs. NO AMD/PBS	ns	0.8501	ns	0.6829	ns	0.99	ns	>0.9999	ns	0.612
Control vs. ROS/PBS	ns	0.4286	ns	0.8451	ns	0.2421	ns	0.9044	ns	0.4335
AMD/PSRA vs. AMD/PBS	ns	>0.9999	ns	0.8677	ns	0.9996	ns	>0.9999	ns	0.9882
AMD/PSRA vs. NO AMD/PBS	ns	0.9625	ns	0.9922	ns	0.953	ns	0.9996	ns	0.9991
AMD/PSRA vs. ROS/PBS	ns	0.6652	ns	0.9998	ns	0.9586	ns	0.8746	ns	0.979
AMD/PBS vs. NO AMD/PBS	ns	0.9671	ns	0.5105	ns	0.9781	ns	>0.9999	ns	0.9469
AMD/PBS vs. ROS/PBS	ns	0.6161	ns	0.692	ns	0.8812	ns	0.895	ns	0.8339
NO AMD/PBS vs. ROS/PBS	ns	0.9276	ns	0.9979	ns	0.7134	ns	0.9449	ns	0.9977

Supplementary Table 4: Data analysis (ANOVA) of the b-wave scotopic 10 cd.d.m² in all different groups.

Tukey's multiple comparisons test	7 Days P = 0.7377		14 Days P = 0.355		30 Days P = 0.6498		60 Days P = 0.6426		90 Days P = 0.7792	
	Significant	Adjusted P Value	Significant	Adjusted P Value	Significant	Adjusted P Value	Significant	Adjusted P Value	Significant	Adjusted P Value
Control vs. AMD/PSRA	ns	0.9994	ns	0.9924	ns	0.906	ns	0.9997	ns	0.881
Control vs. AMD/PBS	ns	>0.9999	ns	0.6591	ns	0.9998	ns	0.9673	ns	0.998
Control vs. NO AMD/PBS	ns	0.9887	ns	0.9835	ns	0.954	ns	>0.9999	ns	>0.9999
Control vs. ROS/PBS	ns	0.9254	ns	0.9924	ns	0.9968	ns	0.6611	ns	>0.9999
AMD/PSRA vs. AMD/PBS	ns	0.9977	ns	0.9414	ns	0.9402	ns	0.9916	ns	0.734
AMD/PSRA vs. NO AMD/PBS	ns	0.9527	ns	0.8993	ns	0.6359	ns	>0.9999	ns	0.9266
AMD/PSRA vs. ROS/PBS	ns	0.9769	ns	0.9277	ns	0.7246	ns	0.7719	ns	0.8586
AMD/PBS vs. NO AMD/PBS	ns	0.9932	ns	0.359	ns	0.9113	ns	0.9862	ns	0.992
AMD/PBS vs. ROS/PBS	ns	0.8757	ns	0.4097	ns	0.9832	ns	0.9366	ns	0.9991
NO AMD/PBS vs. ROS/PBS	ns	0.6597	ns	>0.9999	ns	0.9907	ns	0.7383	ns	0.9997

Supplementary Table 5: Data analysis (ANOVA) of the b-wave photopic 3 cd.d.m² in all different groups.

Tukey's multiple comparisons test	7 Days P = 0.5236		14 Days P = 0.3133		30 Days P = 0.0705		60 Days P = 0.5411		90 Days P = 0.9090	
	Significant	Adjusted P Value	Significant	Adjusted P Value	Significant	Adjusted P Value	Significant	Adjusted P Value	Significant	Adjusted P Value
Control vs. AMD/PSRA	ns	0.6993	ns	>0.9999	ns	0.4391	ns	0.8403	ns	0.2185
Control vs. AMD/PBS	ns	0.9	ns	0.9691	ns	0.7186	ns	0.9966	ns	0.9544
Control vs. NO AMD/PBS	ns	0.9222	ns	0.6464	ns	0.8177	ns	0.9968	ns	0.1008
Control vs. ROS/PBS	ns	0.4449	ns	0.8633	ns	0.2867	ns	0.9634	ns	0.7769
AMD/PSRA vs. AMD/PBS	ns	0.9882	ns	0.9725	ns	0.9763	ns	0.9456	ns	0.5522

AMD/PSRA vs. NO AMD/PBS	ns	0.9811	ns	0.7874	ns	0.1439	ns	0.9572	ns	0.9896
AMD/PSRA vs. ROS/PBS	ns	0.996	ns	0.9332	ns	0.9994	ns	0.4402	ns	0.8108
AMD/PBS vs. NO AMD/PBS	ns	>0.9999	ns	0.3022	ns	0.2624	ns	>0.9999	ns	0.3093
AMD/PBS vs. ROS/PBS	ns	0.8956	ns	0.5165	ns	0.9109	ns	0.8228	ns	0.9901
NO AMD/PBS vs. ROS/PBS	ns	0.8681	ns	0.9937	ns	0.0909	ns	0.8456	ns	0.5488

Supplementary Table 6: Data analysis (ANOVA) of the a-wave scotopic 3.0 cd.d.m² in all different groups.

Tukey's multiple comparisons test	7 Days P = 0.0993		14 Days P = 0.0811		30 Days P = 0.1317		60 Days P = 0.2491		90 Days P = 0.0416*	
	Significant	Adjusted P Value	Significant	Adjusted P Value	Significant	Adjusted P Value	Significant	Adjusted P Value	Significant	Adjusted P Value
Control vs. AMD/PSRA	ns	0.8139	ns	0.2345	ns	>0.9999	ns	0.9686	ns	0.9909
Control vs. AMD/PBS	ns	0.9103	ns	0.9247	ns	0.2062	ns	0.949	ns	0.9999
Control vs. NO AMD/PBS	ns	0.2555	ns	0.7255	ns	0.8766	ns	0.7433	ns	0.1004
Control vs. ROS/PBS	ns	0.0967	ns	0.9955	ns	0.3889	ns	0.9561	ns	0.321
AMD/PSRA vs. AMD/PBS	ns	0.9984	ns	0.0674	ns	0.2308	ns	0.6473	ns	0.9735
AMD/PSRA vs. NO AMD/PBS	ns	0.8616	ns	0.8081	ns	0.8981	ns	0.9751	ns	0.212
AMD/PSRA vs. ROS/PBS	ns	0.5504	ns	0.3786	ns	0.4264	ns	0.6654	ns	0.5578
AMD/PBS vs. NO AMD/PBS	ns	0.6703	ns	0.2813	ns	0.9101	ns	0.3072	ns	0.0767
AMD/PBS vs. ROS/PBS	ns	0.3332	ns	0.7611	ns	0.9896	ns	>0.9999	ns	0.2579
NO AMD/PBS vs. ROS/PBS	ns	0.9736	ns	0.9034	ns	0.986	ns	0.3211	ns	0.9476

Supplementary Table 7: Data analysis (ANOVA) of the a-wave scotopic 10 cd.d.m² in all different groups.

Tukey's multiple comparisons test	7 Days P = 0.4264		14 Days P = 0.0264*		30 Days P = 0.0182*		60 Days P < 0.0001****		90 Days P = 0.4794	
	Significant	Adjusted P Value	Significant	Adjusted P Value	Significant	Adjusted P Value	Significant	Adjusted P Value	Significant	Adjusted P Value

Control vs. AMD/PSRA	ns	0.9998	ns	0.7315	ns	0.992	ns	>0.9999	*	0.0462
Control vs. AMD/PBS	ns	0.944	ns	0.994	ns	0.9928	ns	>0.9999	ns	0.393
Control vs. NO AMD/PBS	ns	0.979	ns	0.9892	ns	0.9991	ns	0.9526	ns	0.9994
Control vs. ROS/PBS	ns	0.7778	ns	0.9777	ns	0.4469	ns	0.8869	ns	0.9256
AMD/PSRA vs. AMD/PBS	ns	0.9785	ns	0.5251	ns	>0.9999	ns	>0.9999	**	0.0014
AMD/PSRA vs. NO AMD/PBS	ns	0.9948	ns	0.4914	ns	>0.9999	ns	0.953	*	0.0303
AMD/PSRA vs. ROS/PBS	ns	0.8624	ns	0.9438	ns	0.7101	ns	0.8877	**	0.0099
AMD/PBS vs. NO AMD/PBS	ns	0.9997	ns	>0.9999	ns	>0.9999	ns	0.9234	ns	0.5153
AMD/PBS vs. ROS/PBS	ns	0.9919	ns	0.8635	ns	0.6438	ns	0.8313	ns	0.8388
NO AMD/PBS vs. ROS/PBS	ns	0.969	ns	0.8335	ns	0.7885	ns	0.9998	ns	0.9762

Supplementary Table 8: Data analysis (ANOVA) of the a-wave photopic 3.0 cd.s.m² in all groups.

ERG values for the AMD/PSRA group showed significant differences between the AMD/PSRA group and the AMD/PBS through 7-90 days (supplementary tables 2, 8 and Figure 1, 3, 4).

Similarly, there was no recovery of the ERG in the AMD/PBS group during the entire period.

Figure 3: ERG values at diverse intensities in AMD/PSRA group. The ERG were done before any experiments (baseline) as a positive control, thirty days after retro-orbital sinus injection of sodium iodate (NaIO₃) as a negative control, seven days after PSRA injection into subretinal space 7, 14, 30, and 90 days after PSRA transplantation. The X-axis is ms/div and Y-axis is μV/div.

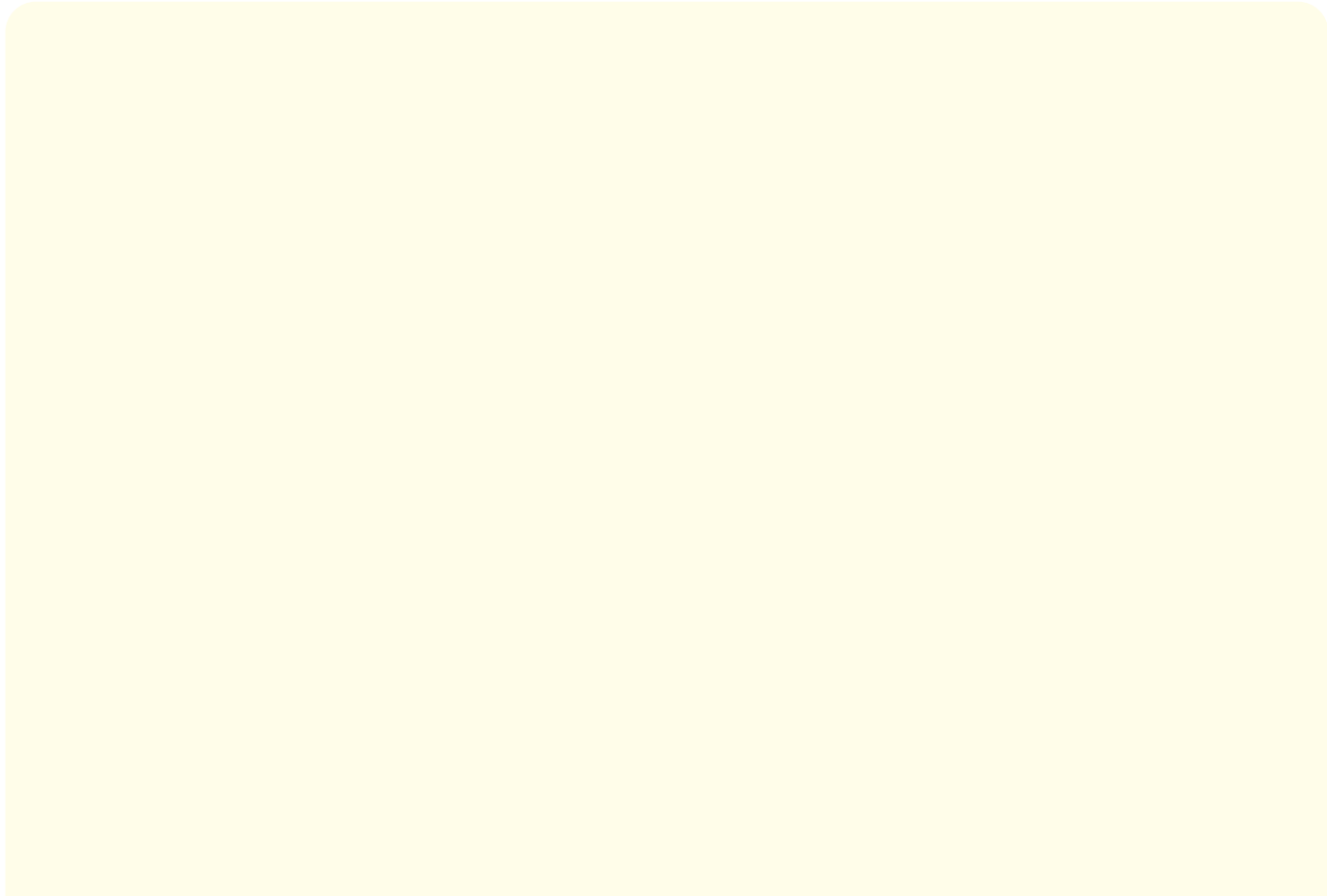


Figure 4: Quantification of full-field ERG obtained in dark and light adaptation to estimate the amplitude of the b- and a-waves in the AMD/PSRA group on different days. Error bars, SEM for 5 rats in each group (*p < 0.05, **p < 0.01, ***p < 0.001, ****p < 0.0001).

Immunohistochemistry

Fate of transplanted PSRA

Immunohistochemistry (IHC) of the AMD/PSRA group showed that PSRA cells had migrated and become incorporated into the host RPE sheet (7 days post-transplantation) (Figure 5). Secondary anti-body Alexa Fluor 594 staining indicated that the grafted PSRA nucleus was labeled with BrdU (7-90 days). The data show transplanted cells (with red nucleus) had integrated into the host cell layer expressing cytoplasmic RPE65. This finding was confirmed at 30, 60, and 90 days post-transplantation.

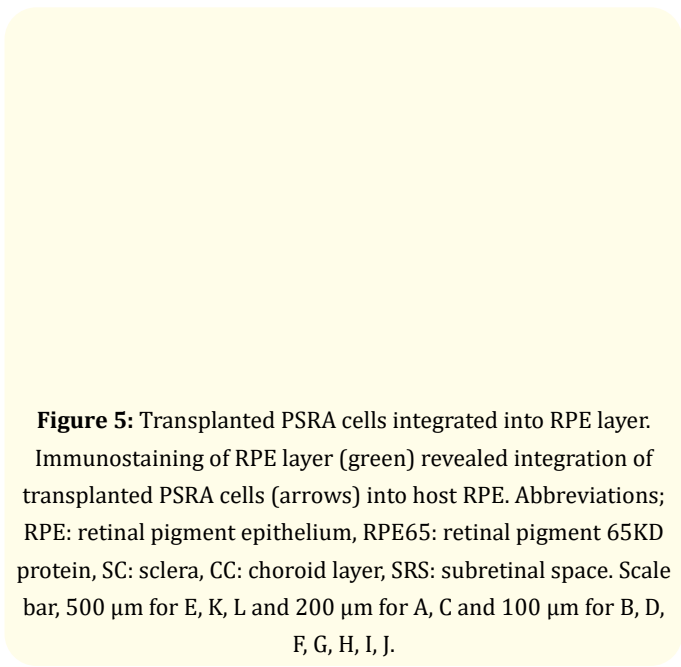


Figure 5: Transplanted PSRA cells integrated into RPE layer. Immunostaining of RPE layer (green) revealed integration of transplanted PSRA cells (arrows) into host RPE. Abbreviations; RPE: retinal pigment epithelium, RPE65: retinal pigment 65KD protein, SC: sclera, CC: choroid layer, SRS: subretinal space. Scale bar, 500 µm for E, K, L and 200 µm for A, C and 100 µm for B, D, F, G, H, I, J.

Immunohistochemistry of retinal flat mounts

At 7-days post-transplantation, there was a small number of hexagonal BrdU-positive red nuclei between host RPE cells expressing RPE65 (Figure 6). At 14-days, there was a greater number of graft-expressing BrdU-positive cells and tight junction protein “ZO-1.” Findings at 14, 30, 60, and 90 days were similar to those of 7 days.

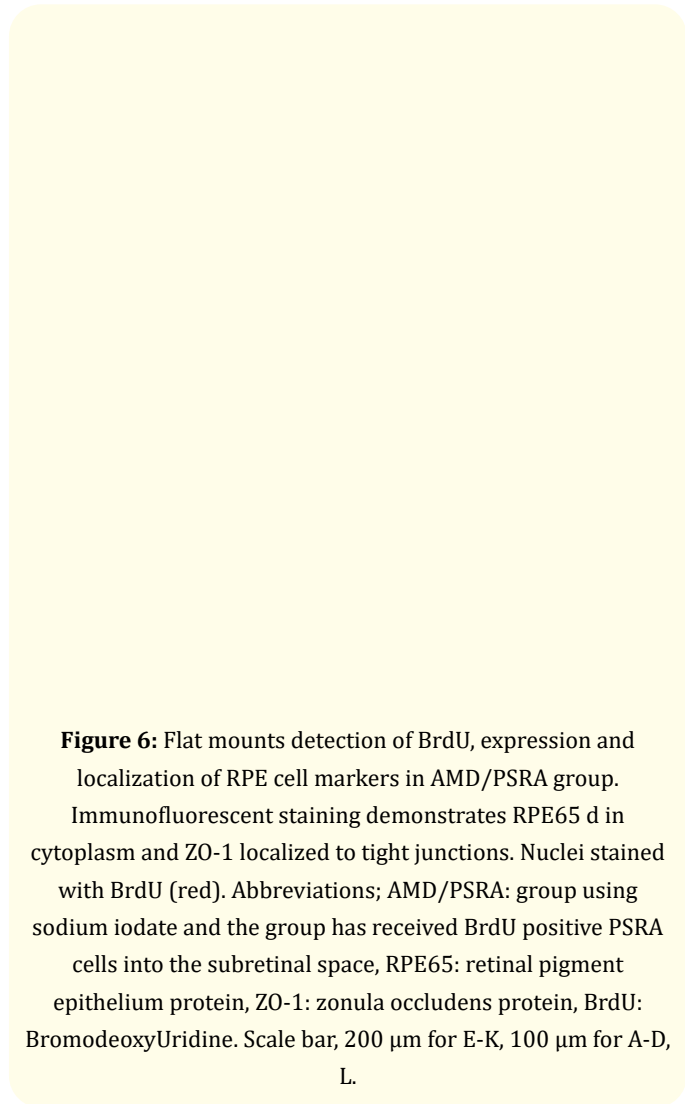


Figure 6: Flat mounts detection of BrdU, expression and localization of RPE cell markers in AMD/PSRA group. Immunofluorescent staining demonstrates RPE65 d in cytoplasm and ZO-1 localized to tight junctions. Nuclei stained with BrdU (red). Abbreviations; AMD/PSRA: group using sodium iodate and the group has received BrdU positive PSRA cells into the subretinal space, RPE65: retinal pigment epithelium protein, ZO-1: zonula occludens protein, BrdU: BromodeoxyUridine. Scale bar, 200 μm for E-K, 100 μm for A-D, L.

Statistical analysis of retinal histology

Statistical analysis of ONL cell count and thickness (Supplementary tables 10-13) indicated a significance differences between ONL count and thickness. There was no significant difference between the control and ROS/PBS groups (Figure 7, 8). There were significant differences between ONL thicknesses in all groups, but there was no difference between the control and NO AMD/PBS, control versus. ROS/PBS (Figure 5, 7).



Figure 7: Quantification of ONL cell count and thickness in AMD/PSRA and other groups. Error bars, SEM for five rats in each group (*p < 0.05, **p < 0.01, ***p < 0.001, ****p < 0.0001).

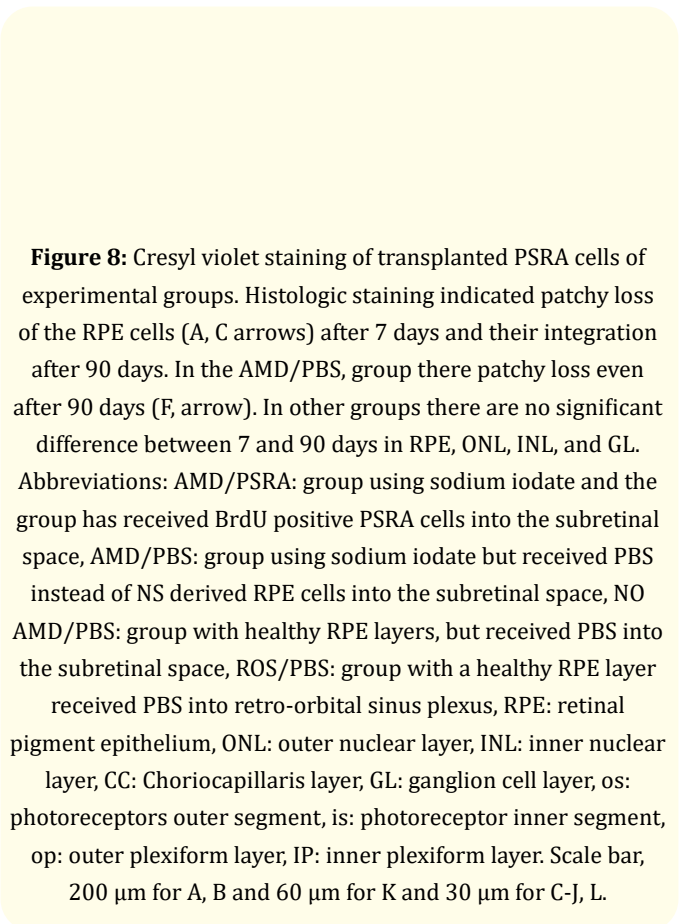


Figure 8: Cresyl violet staining of transplanted PSRA cells of experimental groups. Histologic staining indicated patchy loss of the RPE cells (A, C arrows) after 7 days and their integration after 90 days. In the AMD/PBS, group there patchy loss even after 90 days (F, arrow). In other groups there are no significant difference between 7 and 90 days in RPE, ONL, INL, and GL. Abbreviations: AMD/PSRA: group using sodium iodate and the group has received BrdU positive PSRA cells into the subretinal space, AMD/PBS: group using sodium iodate but received PBS instead of NS derived RPE cells into the subretinal space, NO AMD/PBS: group with healthy RPE layers, but received PBS into the subretinal space, ROS/PBS: group with a healthy RPE layer received PBS into retro-orbital sinus plexus, RPE: retinal pigment epithelium, ONL: outer nuclear layer, INL: inner nuclear layer, CC: Choriocapillaris layer, GL: ganglion cell layer, os: photoreceptors outer segment, is: photoreceptor inner segment, op: outer plexiform layer, IP: inner plexiform layer. Scale bar, 200 μm for A, B and 60 μm for K and 30 μm for C-J, L.

AMD/ RPE group	Scotopic b-wave 0.01 cd.s/m ²		Scotopic b-wave 3.0 cd.s/m ²		Scotopic b-wave 10.0 cd.s/m ²		Photopic b-wave 3.0 cd.s/m ²		Scotopic a-wave 3.0 cd.s/m ²		Scotopic a-wave 10.0 cd.s/m ²		Photopic a-wave 3.0 cd.s/m ²	
7d-14d	ns	0.6056	ns	0.445	ns	0.3119	ns	0.8613	ns	0.2831	*	0.0192 (60.07 ± 17.66)	ns	0.2554
7d-30d	*	0.0273 (52.78 ± 37.24)	*	0.0079 (38.23 ± 68.53)	*	0.0284 (5.900 ± 37.16)	*	0.0433 (3.745 ± 20.59)	**	0.0048 (-29.42 ± 29.39)	*	0.0469 (25.40 ± 10.19)	ns	0.8701
7d-60d	*	0.0465 (77.63 ± 37.58)	ns	0.8477	ns	0.5865	ns	0.6151	ns	0.6602	*	0.0455 (23.58 ± 9.367)	ns	0.7961
7d-90d	ns	0.9359	ns	0.2190	ns	0.3512	ns	0.4984	ns	0.4523	ns	0.5886	**	0.0087 (25.25 ± 6.597)
14d-30d	ns	0.1488	ns	0.0724	*	0.0233 (59.03 ± 39.53)	ns	0.0767	ns	0.0700	ns	0.1599	ns	0.2019
14d-60d	**	0.0020 (102.6 ± 17.39)	ns	0.3000	ns	0.7953	ns	0.5543	ns	0.4523	ns	0.0732	ns	0.3616
14d-90d	ns	0.2030	ns	0.2784	ns	0.2866	ns	0.6681	ns	0.4523	*	0.0121 (62.39 ± 16.26)	ns	0.6173
30d-60d	****	<0.0001 (130.4 ± 11.7)	*	0.0113 (56.41 ± 60.75)	*	0.0105 (22.88 ± 51.87)	*	0.0175 (8.195 ± 27.91)	*	0.0109 (31.65 ± 22.38)	ns	0.6292	ns	0.6742
30d-90d	*	0.0175 (48.08 ± 43.26)	ns	0.0780	ns	0.1455	ns	0.1383	*	0.0109 (31.65 ± 22.38)	*	0.0160 (27.73 ± 8.352)	*	0.0111 (23.23 ± 6.418)
60d-90d	*	0.0300 (-82.33 ± 43.55)	ns	0.2921	ns	0.1557	ns	0.2510	ns	>0.9999	*	0.0123 (25.90 ± 7.331)	*	0.0193 (22.03 ± 6.951)

Supplementary Table 9: Data analysis (Two-tailed t-test) of the b-and a-wave scotopic/ photopic of all intensities in AMD/PSRA group.

Tukey's multiple comparisons test	7 Days P < 0.0001****		14 Days P < 0.0001****		30 Days P < 0.0001****		60 Days P < 0.0001****		90 Days P < 0.0001****	
	Significant	Adjusted P Value	Significant	Adjusted P Value	Significant	Adjusted P Value	Significant	Adjusted P Value	Signifi- cant	Adjusted P Value
Control vs. AMD/PSRA	*	0.0255	ns	0.1834	****	<0.0001	****	<0.0001	****	<0.0001
Control vs. AMD/PBS	****	<0.0001	****	<0.0001	****	<0.0001	****	<0.0001	****	<0.0001

Control vs. NO AMD/PBS	****	<0.0001	****	<0.0001	****	<0.0001	****	<0.0001	****	<0.0001
Control vs. ROS/PBS	ns	0.2552	ns	0.1421	ns	0.1384	ns	0.7329	ns	0.1656
AMD/PSRA vs. AMD/PBS	****	<0.0001	****	<0.0001	****	<0.0001	ns	0.5999	*	0.04
AMD/PSRA vs. NO AMD/PBS	ns	0.3934	****	<0.0001	ns	0.9672	****	<0.0001	****	<0.0001
AMD/PSRA vs. ROS/PBS	ns	0.8403	ns	>0.9999	*	0.016	****	<0.0001	****	<0.0001
AMD/PBS vs. NO AMD/PBS	****	<0.0001	****	<0.0001	****	<0.0001	****	<0.0001	****	<0.0001
AMD/PBS vs. ROS/PBS	****	<0.0001	****	<0.0001	****	<0.0001	****	<0.0001	****	<0.0001
NO AMD/PBS vs. ROS/PBS	ns	0.0508	****	<0.0001	**	0.0024	***	0.0005	*	0.0109

Supplementary Table 10: Data analysis (One-way ANOVA) of ONL cell count in all group.

AMD/PSRA ONL cell count	7d-14d		7d-30d		7d-60d		7d-90d		14d-30d		14d-60d		14d-90d		30d-60d		30d-90d		60d-90d	
P value	ns	0.0683	ns	0.1352	****	<0.0001	****	<0.0001	***	0.0004	****	<0.0001	****	<0.0001	****	<0.0001	****	<0.0001	**	0.0053
Difference between means (B - A) ± SEM	132.5 ± 69.10		-98.33 ± 63.41		-609.3 ± 59.21		-525.0 ± 54.73		-230.8 ± 55.09		-741.8 ± 50.21		-657.5 ± 44.83		-510.9 ± 42.02		-426.7 ± 35.42		84.25 ± 27.21	

Supplementary Table 11: Two tailed t-test analysis of ONL cell count AMD/PSRA group.

Tukey's multiple comparisons test	7 Days P < 0.0001****		14 Days P < 0.0001****		30 Days P < 0.0001****		60 Days P < 0.0001****		90 Days P < 0.0001****	
	Significant	Adjusted P Value	Significant	Adjusted P Value	Significant	Adjusted P Value	Significant	Adjusted P Value	Significant	Adjusted P Value
Control vs. AMD/PSRA	****	<0.0001	ns	0.9584	*	0.0339	****	<0.0001	****	<0.0001
Control vs. AMD/PBS	****	<0.0001	***	0.0005	****	<0.0001	****	<0.0001	****	<0.0001
Control vs. NO AMD/PBS	ns	>0.9999	ns	0.9587	ns	>0.9999	ns	>0.9999	ns	0.9785
Control vs. ROS/PBS	ns	0.814	ns	0.9213	ns	0.9083	ns	0.8625	ns	0.312
AMD/PSRA vs. AMD/PBS	ns	>0.9999	**	0.0045	**	0.0033	ns	0.0555	**	0.0014

AMD/PSRA vs. NO AMD/PBS	****	<0.0001	ns	>0.9999	*	0.0321	****	<0.0001	****	<0.0001
AMD/PSRA vs. ROS/PBS	****	<0.0001	ns	>0.9999	ns	0.2383	****	<0.0001	****	<0.0001
AMD/PBS vs. NO AMD/PBS	****	<0.0001	**	0.0045	****	<0.0001	****	<0.0001	****	<0.0001
AMD/PBS vs. ROS/PBS	****	<0.0001	**	0.007	****	<0.0001	****	<0.0001	****	<0.0001
NO AMD/PBS vs. ROS/PBS	ns	0.7698	ns	>0.9999	ns	0.9009	ns	0.8243	ns	0.658

Supplementary Table 12: Data analysis (One-way ANOVA) of ONL thickness in all group.

AMD/PSRA ONL cell count	7d-14d		7d-30d		7d-60d		7d-90d		14d-30d		14d-60d		14d-90d		30d-60d		30d-90d		60d-90d	
P value	**	0.0057	**	0.0022	ns	0.1281	ns	0.0976	ns	0.3894	*	0.0363	*	0.0151	ns	0.0558	**	0.0087	ns	0.5491
Difference between means (B - A) ± SEM	412093 ± 137660		279344 ± 82847		99459 ± 63420		67338 ± 39294		-132749 ± 151830		-312634 ± 142165		-344754 ± 133164		-179885 ± 90134		-212006 ± 75140		-32120 ± 52959	

Supplementary Table 13: Two tailed *t*-test analysis of ONL thickness AMD/PSRA group.

Within the AMD/PSRA group, marked differences were apparent throughout the 7-90 day period in ONL cell count (Figure 7) and throughout the 14-90 day period in ONL thickness between the AMD/PSRA and the AMD/PBS groups (Figure 7).

At 7-days post-transplantation, cresyl violet staining in AMD/PSRA revealed injury areas, with morphological changes in RPE cells (red arrows) and a disorganized retina. High magnification (x100) revealed that the RPE cells had lost their order, with dark-to-no melanin. At 90-days post-transplantation, the structure of the neurosensory retina and RPE sheet were similar to those of the control. In AMD/PBS group, there was disorganization of RPE cells and neurosensory retina over the 7-90-days post-transplantation. At 7-days post-transplantation, there was a slight increase in ONL cells in the NO AMD/PBS group, but by 90-days, the structure of the retina and RPE sheet were similar to those of the control group. The ROS/PBS group showed no changes in the RPE layer and neurosensory retina (Figure 8).

Discussion

We demonstrated that PSRA migrated into the subretinal space and integrated into the host layer, and as well as expressed ZO-1, a RPE65 marker. We also showed that photoreceptor activity improved, and ONL cell numbers and thickness were preserved.

The rat is a suitable model for investigating the etiology of retinal pathology *in vivo*.

Sodium iodate is a chemical component that affects visual function adversely. It has toxic effects on RPE cells, often leading to necrosis and PR apoptosis [17]. Chondroitinase ABC [18] provides a possible cell migration mechanism to such injured tissue [19]. There are a number of different mechanisms of action of sodium iodate in inducing an RPE degeneration model: (i) effect on cytoplasmic melanosomes, (ii) changes in hydrogen sulfide levels, (iii) inhibition of sulphydryl enzyme activity that result in damage to the retinal-blood barrier, (iv) induction of oxidative stress leading to accumulation of active oxygen species (ROS), (v) inactivation of PTEN and loss of its interactions with junctional proteins, (vi) impairment of the Nrf2 signaling pathway, and (vii) mitochondrial dysfunction [20].

In the present study, we demonstrated that the transplantation of PSRA cells into the subretinal space improved retinal activity. This finding is in alignment with the report that both a- and b-wave amplitudes were significantly higher in rd10 mice that received hiPSC-RPE transplants than in the ungrafted group 9,[21]. Our data show that integrated PSRA cells express specific proteins 90-days post-transplantation. In addition, at this time, retinal activity was improved.

While these results are intriguing, interpretation of the mechanism(s) of photoreceptor rescue after RPE transplantation is not clear-cut. Three systems have been suggested to account for the etiogenesis behind these mechanisms: (i) neurotrophic-releasing factors like bFGF, BDNF, CNTF, IL-6 [22], NT3, NGF, IGF-1 [23], and GL-derived factors; and micro- and nano-lipid microvesicles [24] RPE and photoreceptors cells [25]. Of note is the fact that RPE cells are able to release these factors [25]. Our results suggest that improvement in retinal activity and photoreceptor rescue related to the items.

Induced pluripotent stem cell-derived RPE cells contribute to retinal rescue and increased ONL thickness after cell transplantation. Studies have shown that iPSCs have neuroprotective properties [26]. As mentioned, these cells express RPE-specific proteins 8 months after transplantation, at which time ONL thickness was significantly increased and ERGs showed improvement [27]. Another element critically contributing to structural and behavioral retinal improvement is the integration of transplanted cells into the host tissue. The adult retina does not provide an environment in which transplanted stem cells can easily migrate, integrate, and differentiate [23]. However, our data suggest that PSRA cells that have originated from BMSCs improve RPE integrity and retinal activity 90 days post-transplantation.

In rodents, the corneal ERG originates from different retinal cell activities. Our data show that there was an apparent decline of b-wave amplitude in dim light stimuli (scotopic 0.01 cd.s/m², rod responses) at 30 days but there was a significant difference in recovery at 60 days post-transplantation in the AMD/PSRA group. Others [28] suggest this to be the maximum activity of rod photoreceptors, ON-central depolarizing bipolar cells, and the third-order neurons, AII and A17 amacrine cells and ON ganglion cells in that time. Our results were in line with the studies that showed subretinal space injection of adult stem cells increase b-wave amplitude via a paracrine function [29].

It has been reported that intravitreal injection of rat BMSCs or human ASCs [30] and adult stem cells had no effect on the b-wave amplitude of Sprague-Dawley rats. This finding is closely linked to the property of the ILM acting as a natural barrier, one that prevents stem cells from passing through and, therefore, integrating into the neural retina [23]. Similarly, human bone marrow stromal stem cells and human embryonic stem cells transplanted into the subretinal space of Long-Evans rats showed an increase in a-

and b-wave amplitudes up to 8 weeks post-transplantation [31]. The precise origin of the ERG b-wave remains in dispute, with significant contributions emanating from light-induced activity in glutamatergic interneurons bipolar cells of the ON-center (light increments) [28]. The b-wave is signaling information regarding light-induced electrical activity in retinal cells that are postsynaptic to the photoreceptors. B-waves are also affected by (i) off-center bipolar cells (light decrements), (ii) light-induced activity in third-order retinal neurons (amacrine and ganglion cells) [28], and (iii) bipolar cell-dependent K⁺ currents that affect Muller cells [32].

Another study demonstrated that human umbilical cord stem cells and human bone marrow stem cells that have been injected into the subretinal space act to rescue not only low-level a-wave responses but also mixed b-wave responses, and rod and cone b-wave amplitude, which showed significant rescue after 60 days [22]. This finding is similar to findings of our study, i.e., that the primary activity of mixed rod and cone photoreceptors (a-wave scotopic 3.0 cd.s/m²) and bipolar cells (b-wave scotopic 3.0 cd.s/m²) that make synapses with third neurons [33] was on 7 and 60 days post-transplantation and continued to 90 days (with a noticeable decline at 30 days).

There are remarkable similarities between our study and others that showed combined transplantation of olfactory ensheathing cells and neural stem cells—compared with a single transplantation—enhanced b-wave amplitude 12 weeks after transplantation into the subretinal space of RCS rats [34].

As stimuli are increased, an initial negative a-wave appears, with an increase in the amplitude of the b-wave (70 sc tds = 9.8 sc cd.s/m²) [35]. The a-wave of the ERG is the leading edge of Granit's P-III component, generated extracellularly along the radial path from the cell body of the photoreceptors, which hyperpolarize in response to light [33], thereby reflecting the functional integrity of the photoreceptors [36]. In our study, there was an apparent decline at 30 days, although retinal activity improved 60 days post-transplantation in the AMD/PSRA group. This finding is in line with those of other studies, which showed a- and b-wave amplitudes increasing up to 20 weeks post-transplantation of human bone marrow stromal stem cells into RSC subretinal space, apparently due to exosomes, trophic factors, and immune system modulatory secreted mechanisms [23]. ERGs of different groups suggest that ON-bipolar cell activity in dim light stimuli in AMD/PSRA groups are greater than of other groups.

Similarly, activity of cone photoreceptors in a-wave photopic 3.0 cd.s/m² at 90 days was greater than on other days. Other studies have also shown that as intensity increases (scotopic 10 cd.s/m²), a-waves becomes more evident, and genuine S Cone and M/S Co-expressing cone [37] photoreceptor activities are increased, comparable to our data at 7 and 60 days. The greatest activity of ON-bipolar cells that synapse with S cone photoreceptors after saturation of rod cells in photopic three cd.s/m² and that relay impulses to amacrine and ON ganglion cells was at 60 days.

Our study demonstrated that pigmented spheres reactive to RPE antigen(s) (PSRA) 7days after transplantation undeniably expressed specific RPE cell proteins, e.g., RPE65 and ZO-1. At this time, the ONL also thickened, perhaps as result of both the secretion of cytokines from the degenerated RPE layer and accumulation PSRA in this layer [38]. MacLaren, *et al.* showed that cells that had migrated and integrated into the subretinal space were post-mitotic. In other words, the ontogenetic stage of transplanted cells is essential to successful cell integration [39]. In contrast, factors such as post-injury reaction, immune response, and lack of developmental features are important contributors to the failure of (i) differentiation of transplanted cells into appropriate cell types and (ii) integration of these cells into surrounding cells [40]. The two major termination points of our transplanted cells were RPE and ONL. However, another a study showed that the ONL, INL, and RPE were the three common destinations in cell replacement therapy [41]. Although there is evidence indicating that the subretinal space is the final destination of transplanted BMSCs [42], there are data to suggest that human embryonic stem cells that have been transplanted into the subretinal space become differentiated into functional retinal cells with improved light responses [42]. Such cells were shown to express photoreceptors specific protein and rhodopsin, and underwent differentiation into PE cells [43], just as we demonstrated in our study. Such cells survived after 4 wk, expressing RPE cell markers [44] throughout 8 mo post-transplantation, with no evidence of tumor formation or inflammation [45]. As in our study, there was increased ONL thickness as well as improvement in RCS activity and generation of lamellar bodies in the cytoplasm of transplanted cells [46]. Two possibilities for the increase in the number of ONL cells: migration of endogenous cells and surgical procedures [47]. Our finding is consistent with those of an earlier report i.e., cell migration into the ONL, INL, and RPE layers [41].

At 14 days post-transplantation, examination of whole-mounts revealed transplanted hexagonal RPE-like cells, findings that are in line with those of previous studies [41]. AT that time, increases in the cell number and thickness of the ONL were prominent. BMSC were able to spare ONL cell apoptosis in a light degenerated model [42] and an RCS rat model [24], improving rod and cone photoreceptor activity as well increasing neurotrophic factors at the site of injection [24]. In our study, we observed an increase in ONL cell number and thickness, with ERGs showing an increase in the b-wave scotopic 10 cd.s/m² and a-wave photopic 3 cd.s/m² in the AMD/PBS group. In contrast to our results, some researchers reported a decrease in ERG amplitude 2 weeks post- subretinal transplantation of human retinal progenitor cells in C57BL/J6 mice, attributing this to the (i) separation of the retina from RPE cells [48] or to (ii) light and transient reduction in ERG b-wave amplitude of human bone marrow mesenchymal stem cells in RCS rats [24]. It appears that the activity of cone photoreceptors is greater than that of rod photoreceptors at this time. Another study found that the b-wave increased two-fold over that of the control group 18 days after BMSCs transplantation [49].

Our study examined several specific RPE cells proteins (RPE65, and ZO-1) on RPE whole-mounts and the IHC following cell transplantation, determining our findings to be consistent with those of a report that demonstrated expression of Mitf and RPE65 in transplanted BMSCs in a sodium iodate model. These cells formed a monolayer on BM [50]. Others have shown that intravitreal injection of BMSCs in a laser-injured retina acted to improve ONL thickness 7 weeks after transplantation [50]. Our study showed that ONL cell number and thickness decreased in the AMD/PSRA group after 30 days, compared to the control group. However, there was an apparent decline in ERG at 30 days, indicating that rod and cone photoreceptor cell activity had declined.

Data collected at 60 days indicated a decrease in both ONL cell count and thickness in the AMD/PSRA group. However, ONL thickness was similar to that of the AMD/PBS group, i.e., ONL cell count increased and ERG amplitude had risen (b-wave amplitude and a-wave scotopic 3.0 cd.s/m²). This finding is in agreement with that of other investigators, suggesting that human BMSC-derived RPE cells were capable of improving both a- and b-wave amplitudes 8-wk post-cell transplantation [31]. These results indicate greater activity of rods, cones, and ON-central bipolar cells, with synapses

between them in the IPL. At 90 days, ONL cells increased in number, but not thickness, in the AMD/PSRA group. However, both number and thickness were increased compared to those of the AMD/PBS group.

The most significant increase in ERG amplitude was related to the b-wave scotopic 0.01 cd.s/m² and a-wave photopic 3.0 cd.s/m², while others showed a decline in b-wave amplitude and increase in maximal a-wave amplitude after 22 weeks and 4-16 weeks post-transplantation respectively [24]. This means that rod and cone photoreceptors are active. Our study showed that the ERG of the AMD/PSRA group after 60 and 90 days had increased in the b-wave scotopic 0.01 cd.s/m² and a-wave photopic 3.0 cd.s/m² compared to the AMD/PBS, NO AMD/PBS, and ROS/PBS groups although, all ERG intensities had increased at 60 and 90 days in the AMD/PSRA group. Other researchers also showed that both a- and b-wave amplitudes increase after RPE transplantation [14]. We proposed the hypothesis that transplanted PSRA cells or ONL cell division are responsible for increasing the ERG value. Perhaps PSRA cells are able to increase the b- and a-wave amplitudes.

Conclusion

We demonstrated that transplantation of PSRA cells into the subretinal space improves retinal activity. Our data suggested that 3-mo post-transplantation, the PSRA cells that integrated into the host layer expressed specific proteins and were associated with improved retinal activity. While these results are intriguing, photoreceptor rescue mechanisms after RPE transplantation are not straightforward. Our data suggest that PSRA cells originating from BMSCs could improve RPE integrity and retinal activity 90 days after transplantation, but treatments for AMD will undoubtedly need to consider other factors. Our data add further support to the understanding that alterations in the diverse stem cells sources (BMSCs, ESCs, and iPSCs) can induce changes in the RPE layer and neurosensory retina.

Acknowledgement

The authors are grateful to Prof. Lawrence Rizzolo, Department of Anatomy and Surgery, Yale University School of Medicine, New Haven, CO, USA, for his support. Funds for this projects were made possible by Shefa Neuroscience Research Center, Khatam Alanbia Hospital, Tehran, Iran (Grant # 86-N-105). The authors are also grateful for the support of the Faculty of Medical Sciences, Tarbiat Modares University, Tehran, Iran.

Disclosure Statement

The authors declare no competing interest.

Availability of Data

Data available within the article or its supplementary materials.

Data Statement

The authors confirm that the data supporting the findings of this study are available within the article (and/or) its supplementary materials.

Bibliography

1. Chan CM., *et al.* "Reactive oxygen species-dependent mitochondrial dynamics and autophagy confer protective effects in retinal pigment epithelial cells against sodium iodate-induced cell death". *Journal of Biomedical Science* 26.1 (2019): 40.
2. Gong J., *et al.* "Stem cell-derived retinal pigment epithelium from patients with age-related macular degeneration exhibit reduced metabolism and matrix interactions". *Stem Cells Translational Medicine* 9.3 (2020): 364-376.
3. Chen X., *et al.* "Unstimulated, serum-free cultures of retinal pigment epithelium excrete large mounds of drusen-like deposits". *Current Eye Research* (2020): 1-5.
4. Fields MA., *et al.* "Extracellular matrix nitration alters growth factor release and activates bioactive complement in human retinal pigment epithelial cells". *PloS One* 12.5 (2017).
5. Fields M., *et al.* "Interactions of the choroid, Bruch's membrane, retinal pigment epithelium, and neurosensory retina collaborate to form the outer blood-retinal-barrier". *Progress in Retinal and Eye Research* (2019): 100803.
6. Naylor A., *et al.* "Tight junctions of the outer blood retina barrier". *International Journal of Molecular Sciences* 21.1 (2020): 211.
7. Blenkinsop TA., *et al.* "Human adult retinal pigment epithelial stem cell-derived RPE monolayers exhibit key physiological characteristics of native tissue". *Investigative Ophthalmology and Visual Science* 56.12 (2015): 7085-7099.
8. Du W., *et al.* "Protection of kaempferol on oxidative stress-induced retinal pigment epithelial cell damage". *Oxidative Medicine and Cellular Longevity* 2018 (2018).

9. Zhu D., *et al.* "Protective effects of human iPS-derived retinal pigmented epithelial cells on retinal degenerative disease". *Stem Cell Research and Therapy* 11.1 (2020): 1-15.
10. Park SS., *et al.* "Advances in bone marrow stem cell therapy for retinal dysfunction". *Progress in Retinal and Eye Research* 56 (2017): 148-165.
11. Kadkhodaeian HA., *et al.* "Generation of Retinal Pigmented Epithelium-Like Cells from Pigmented Spheres Differentiated from Bone Marrow Stromal Cell-Derived Neurospheres". *Tissue Engineering and Regenerative Medicine* 16.3 (2019): 253-263.
12. Kadkhodaeian HA., *et al.* "High efficient differentiation of human adipose-derived stem cells into retinal pigment epithelium-like cells in medium containing small molecules inducers with a simple method". *Tissue and Cell* 5.6 (2019): 52-59.
13. Aboutaleb HK., *et al.* "Survival and Migration of Adipose-Derived Stem Cells Transplanted in the Injured Retina". *Experimental and Clinical Transplantation: Official Journal of the Middle East Society for Organ Transplantation* (2017).
14. Koster C., *et al.* "A Systematic Review on Transplantation Studies of the Retinal Pigment Epithelium in Animal Models". *International Journal of Molecular Sciences* 21.8 (2020): 2719.
15. Kadkhodaeian HA., *et al.* "Histological and electrophysiological changes in the retinal pigment epithelium after injection of sodium iodate in the orbital venus plexus of pigmented rats". *Journal of Ophthalmic and Vision Research* 11.1 (2016): 70.
16. Qi Y., *et al.* "Trans-corneal subretinal injection in mice and its effect on the function and morphology of the retina". *PLoS One* 10.8 (2015).
17. Liu Y., *et al.* "Morphologic and histopathologic change of sodium iodate-induced retinal degeneration in adult rats". *International Journal of Clinical and Experimental Pathology* 12.2 (2019): 443.
18. Ma J., *et al.* "Combining chondroitinase ABC and growth factors promotes the integration of murine retinal progenitor cells transplanted into Rho-/- mice". *Molecular Vision* 17 (2011): 1759.
19. Imitola J., *et al.* "Directed migration of neural stem cells to sites of CNS injury by the stromal cell-derived factor 1 α /CXCL12 chemokine receptor 4 pathway". *Proceedings of the National Academy of Sciences* 101.52 (2004): 18117-18122.
20. Kaarniranta K., *et al.* "Mechanisms of mitochondrial dysfunction and their impact on age-related macular degeneration". *Progress in Retinal and Eye Research* (2020): 100858.
21. Lin TC., *et al.* "Assessment of safety and functional efficacy of stem cell-based therapeutic approaches using retinal degenerative animal models". *Stem Cells International* 2017 (2017).
22. Lund RD., *et al.* "Cells isolated from umbilical cord tissue rescue photoreceptors and visual functions in a rodent model of retinal disease". *Stem Cells* 25.3 (2007): 602-611.
23. Puertas-Neyra K., *et al.* "Intravitreal stem cell paracrine properties as a potential neuroprotective therapy for retinal photoreceptor neurodegenerative diseases". *Neural Regeneration Research* 15.9 (2020): 1631.
24. Tzameret A., *et al.* "Epiretinal transplantation of human bone marrow mesenchymal stem cells rescues retinal and vision function in a rat model of retinal degeneration". *Stem Cell Research* 15.2 (2015): 387-394.
25. Comyn O., *et al.* "Induced pluripotent stem cell therapies for retinal disease". *Current Opinion in Neurology* 23.1 (2010): 4.
26. Harvey JP., *et al.* "Induced Pluripotent Stem Cells for Inherited Optic Neuropathies-Disease Modeling and Therapeutic Development". *Journal of Neuro-ophthalmology: The Official Journal of the North American Neuro-ophthalmology Society* (2021).
27. Marchetti V., *et al.* "Stemming vision loss with stem cells". *The Journal of Clinical Investigation* 120.9 (2010): 3012-3021.
28. Park SJ., *et al.* "Convergence and divergence of CRH amacrine cells in mouse retinal circuitry". *Journal of Neuroscience* 2018. 38 (15): 3753-3766.
29. Hu C., *et al.* "Transplantation Site Affects the Outcomes of Adipose-Derived Stem Cell-Based Therapy for Retinal Degeneration". *Stem Cells International* 2020 (2020).
30. Huang H., *et al.* "Intravitreal injection of mesenchymal stem cells evokes retinal vascular damage in rats". *The FASEB Journal* 33.12 (2019): 14668-14679.
31. Duan P., *et al.* "Comparison of protective effects of hESCs-derived and hBMSCs-derived RPE cells on sodium iodate-injured rat retina". *International Journal of Clinical and Experimental Pathology* 10.5 (2017): 5274-5284.

32. Saszik SM, et al. "The scotopic threshold response of the dark-adapted electroretinogram of the mouse". *The Journal of Physiology* 543.3 (2002): 899-916.
33. Panse M. "Analysis of bioelectrical signal of the human retina (ERG) using LabVIEW". in 2010 IEEE Students Technology Symposium (TechSym). IEEE (2010).
34. Zhai W, et al. "Combined transplantation of olfactory ensheathing cells with rat neural stem cells enhanced the therapeutic effect in the retina of RCS rats". *Frontiers in Cellular Neuroscience* 14 (2020): 52.
35. Robson J, et al. "In vivo studies of signaling in rod pathways of the mouse using the electroretinogram". *Vision Research* 44.28 (2004): 3253-3268.
36. Perlman I. "The electroretinogram: ERG". in *Webvision: The Organization of the Retina and Visual System*. 2007, University of Utah Health Sciences Center (2007).
37. Demb JB and JH Singer. "Functional circuitry of the retina". *Annual Review of Vision Science* 1 (20195): 263-289.
38. Chacko DM, et al. "Transplantation of ocular stem cells: the role of injury in incorporation and differentiation of grafted cells in the retina". *Vision Research* 43.8 (2003): 937-946.
39. Chen X, et al. "Adult limbal neurosphere cells: a potential autologous cell resource for retinal cell generation". *Plos One* 9.10 (2014).
40. Hertz J, et al. "Survival and integration of developing and progenitor-derived retinal ganglion cells following transplantation". *Cell Transplantation* 23.7 (20194): 855-872.
41. Tomita, M, et al. "Bone marrow-derived stem cells can differentiate into retinal cells in injured rat retina". *Stem Cells* 20.4 (2002): 279-283.
42. Zhang Y and W Wang. "Effects of bone marrow mesenchymal stem cell transplantation on light-damaged retina". *Investigative Ophthalmology and Visual Science* 51.7 (2010): 3742-3748.
43. Stern JH and S Temple. "Stem cells for retinal replacement therapy". *Neurotherapeutics* 8.4 (2011): 736-743.
44. Park UC, et al. "Subretinal transplantation of putative retinal pigment epithelial cells derived from human embryonic stem cells in rat retinal degeneration model". *Clinical and Experimental Reproductive Medicine* 38.4 (2011): 216-221.
45. Lund RD, et al. "Subretinal transplantation of genetically modified human cell lines attenuates loss of visual function in dystrophic rats". *Proceedings of the National Academy of Sciences* 98.17 (2001): 9942-9947.
46. Lund RD, et al. "Human embryonic stem cell-derived cells rescue visual function in dystrophic RCS rats". *Cloning and Stem Cells* 8.3 (2006): 189-199.
47. Lu B, et al. "Neural stem cells derived by small molecules preserve vision". *Translational Vision Science and Technology* 2.1 (2013): 1-1.
48. Huang R, et al. "Functional and morphological analysis of the subretinal injection of human retinal progenitor cells under Cyclosporin A treatment". *Molecular Vision* 20 (2014): 1271.
49. Harris JR, et al. *Stem Cells* 27.2 (2011): 457-466.
50. Chung JK, et al. "Modulation of retinal wound healing by systemically administered bone marrow-derived mesenchymal stem cells". *Korean Journal of Ophthalmology* 25.4 (2011): 268-274.